

Synthesis of nanosized $(1-x)\text{BiScO}_3-x\text{PbTiO}_3$ ferroelectric ceramic powders

Wei Zhao · Xiaohui Wang · Longtu Li · Zhilun Gui

Published online: 20 August 2007
© Springer Science + Business Media, LLC 2007

Abstract Nanosized $(1-x)\text{BiScO}_3-x\text{PbTiO}_3$ ferroelectric ceramic powders was obtained by the metal citrate sol–gel method. The decomposition process of the polymer was studied by using infrared spectral absorption and X-ray diffraction. Perovskite phase can be obtained at the calcining temperature as low as 450 °C and the average grain sizes of powders were calculated by XRD method. The influence of the grain size by pH value of the solution is explained. The calcining temperature is proved to be the foremost factor to determine the grain size which grew from 12 to 23 nm when calcined at different temperatures. The holding time can also affect the grain size. The sintering temperature can be reduced by 100 °C using nano powders than using traditionally prepared large grain powders.

Keywords Ferroelectric ceramic powders · XRD method · Perovskite phase

1 Introduction

The $(1-x)\text{BiScO}_3-x\text{PbTiO}_3$ solid solution, as a member of the system $(1-x)\text{Bi}(\text{Me})\text{O}_3-x\text{PbTiO}_3$ (where Me is usually a large cation, Sc, Y, Yb, In etc.) was firstly introduced by EITEL et al. [1, 2]. As most of the PT solid solution system,

this system (use BSPT for short) also has a morphotropic phase boundary (MPB) where the dielectric and piezoelectric properties are enhanced. The most promising trait for this system is that it has both high piezoelectric coefficient and high Curie temperature. For the large-grain ceramics prepared by conventional method, the piezoelectric coefficient d_{33} is 450 pC/N and the Curie temperature is 450 °C at MPB. However, Iniguez et al. [3] pointed out that the BSPT's intrinsic piezoelectric property may be beyond the experimental value to date. Besides, the high T_c indicates that these kinds of materials could be applied in high temperature environment such as sensors of automobiles' motors. In recent years, different methods were used to improve the piezoelectric properties [4–8] for this series of materials. Owing to the piezoelectric properties could be enhanced by reducing the grain size of the ceramics, we aimed at using nano-grain powders to obtain small-grain ceramics.

Another motivation for us to study the preparation is that as the ferroelectric device elements become smaller and smaller the properties become size-dependent and the grain size effect becomes one of the most important factors to optimize the properties [9]. To study the size effect of the piezoelectric ceramics, preparing samples with small grains where size effect could be presented is still a challenge. Since the foremost factor to determine the grain size of ceramics is the sintering temperature, we choose BSPT system to study for it has relatively low sintering temperature which could be further reduced by using nano powder. Hence, the preparation of nano powders is the first step for the purpose.

In order to minimize the grain size, the factors which may influence the sizes were studied. The probable factors are as follow: the concentration and pH value of the solutions, the heat treatment temperature for the solution,

W. Zhao · X. Wang (✉) · L. Li · Z. Gui
State Key lab of New Ceramics and Fine Processing,
Department of Material Science and Engineering,
Tsinghua University,
Beijing 100084, People's Republic of China
e-mail: wxh@mail.tsinghua.edu.cn

the calcining temperature and holding time for the dried gel. As we found, the concentration and heat treatment of the solution before calcination are not important. The factors which could influence the grain size and the effects of those factors will be discussed later.

2 Experimental methods

2.1 Powder preparation

The starting materials were $\text{Pb}(\text{Ac})_2 \cdot 3\text{H}_2\text{O}$, $\text{Bi}(\text{NO}_3)_3 \cdot 5\text{H}_2\text{O}$, $\text{Ti}(\text{OC}_4\text{H}_9)_4$, Sc_2O_3 , citric acid ($\text{C}_6\text{H}_8\text{O}_7$), ammonia ($\text{NH}_3 \cdot \text{H}_2\text{O}$) and nitric acid (HNO_3), all of the which were analytical reagent. Firstly, Sc_2O_3 was dissolved into nitric acid aqueous solution, then $\text{Bi}(\text{NO}_3)_3 \cdot 5\text{H}_2\text{O}$ was added into the solution. Citric acid solution was prepared separately, and was added with ammonia to adjust pH value. After that, the two solutions were mixed together and $\text{Ti}(\text{OC}_4\text{H}_9)_4$, $\text{Pb}(\text{Ac})_2 \cdot 3\text{H}_2\text{O}$ were then dissolved into the solution. In the whole preparing process, the pH value for each step must be controlled strictly to avoid hydrolysis. Solutions with different pH value were prepared to investigate the effects of pH value for decomposition process and the final grain sizes. The solution was dried at 120 °C to form a stable gel. The gel was then heated at 200 °C and it swelled to a bread-like mass which we called dried gel. The dried gel has a very large expansion ratio and a great deal of air pores in it. The nano powders with different grain sizes could be obtained by calcining the dried gel at different temperatures and holding times. To investigate the dependence of grain size on temperature, powders with different components were calcined at the temperatures from 500 to 800 °C with the interval of 100 °C. Powders heated for 3, 8 and 16 h at 600 °C were used to determine the holding time dependence of grain size.

2.2 Characterization

TG-DTG curves of the dried gel were taken by TGA2050 to indicate the decomposition course in the calcining process. The infrared spectral absorption (IR) spectra of different powders obtained at different steps of the decomposition were recorded by Spectrum GX. They were used to analyze the organic products in those powders. X-ray diffraction (XRD) patterns were taken by using a diffractometer (Japan, Rigaku, D/max-RB) with $\text{Cu K}\alpha$ radiation. For deriving the mean particle size of the powders, the half-value widths of the XRD peaks of those powders were measured by step scan and the sizes were calculated in terms of Scherrer's equation. Patterns by continuous scan between 20 and 60° were used to determine the phase structures.

3 Results and discussion

3.1 Decomposition process

The TG-DTG curves of the dried gel are shown in Fig. 1. The curves show that the decomposition process terminated at 530 °C and there are three decomposition peaks at 275, 355 and 530 °C. The XRD patterns of the powders calcined at 300, 450 and 530 °C are shown in Fig. 2. According to the pattern (a), no metal oxide existing in the powder indicates that the metal citric complex hadn't decomposed at 275 °C. When the powder was calcined at 355 °C, an auto-combustion process began to occur, but this process couldn't accomplish completely. Some of the powder burned and turned to yellow while some of them remained brown or black. The combustion went on with the temperature increasing. Figure 3 shows the IR spectra of the powders (a) unburned and (b) burned at 380 °C. As the spectra show, the peak at 618 cm^{-1} which belongs to the oxide absorption indicates the formation of the perovskite. The wide gaps between 900 and $1,700 \text{ cm}^{-1}$ and between 1,700 and $3,600 \text{ cm}^{-1}$ in Fig. 3(a) derive from the polymer molecules with different molecular weights. The molecules were produced from the bonding of hydroxyl and carboxyl in citric acid. Those gaps became smaller and shallower in Fig. 3(b), corresponding to the auto-combustion of the powder. The XRD pattern in Fig. 2(b) shows that perovskite phase formed in the burned powder after combustion. The powders prepared by the solutions with different pH values show different auto-combustion possibilities. Solutions with pH of 3 and 4 could combust more easily and that would cause a little difference of grain sizes. The organic products can be eliminated by calcining the powder at 530 °C, as shown in Fig. 3(c). The remnant small gaps are due to the trace remnant of organic matter. The XRD pattern of this powder is shown in Fig. 2(c).

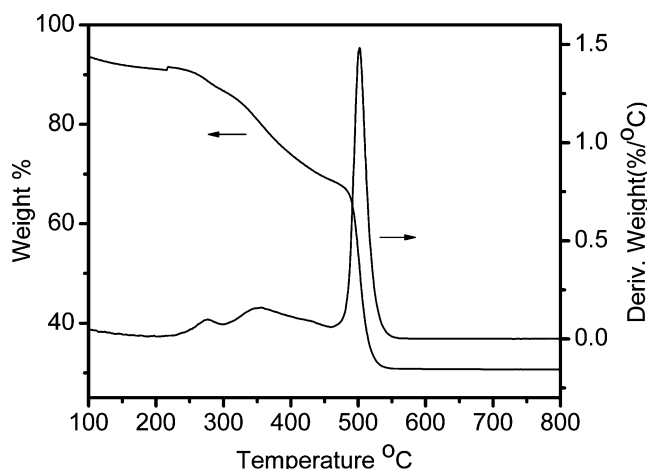


Fig. 1 TG-DTG curve of the dried gel (for tetragonal phase component and pH=5.5)

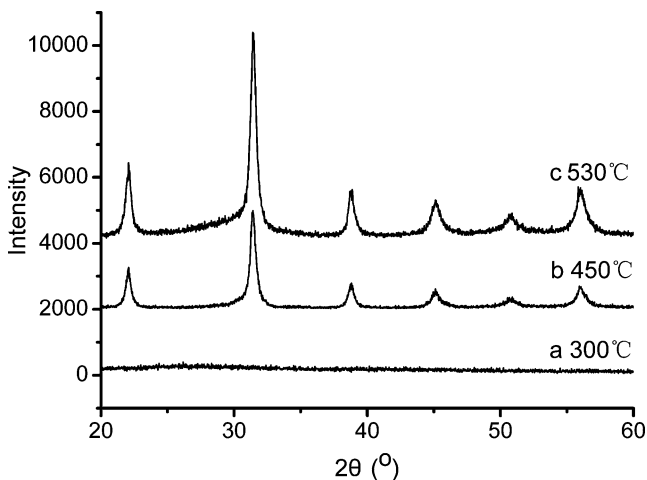


Fig. 2 XRD patterns of powders with different calcining temperatures. (a) Calcined at 300 °C for 3 h (b) burned powder calcined at 450 °C for 3 h (c) calcined at 530 °C for 3 h

3.2 Dependences of the grain size

The grain sizes of calcined ceramic powders prepared by solutions with different pH values are shown in Fig. 4. The solutions with smaller pH value between 3 and 6 have smaller grain sizes. The influence by pH value was discussed as above when analyzing the decomposition process.

Grain sizes of powders calcined at different temperatures are shown in Fig. 5. The result shows that the calcining temperature is the most important factor to determine the grain size. It grew from 12 to 23 nm in average as the calcining temperature rose from 500 to 800 °C. However, the original grain size is determined by the temperature of the self-combustion. As shown in Fig. 5, the grain size of the powders calcined at 500 and 600 °C are nearly the same. So it is not feasible to obtain smaller grain size simply by reducing the calcining temperature.

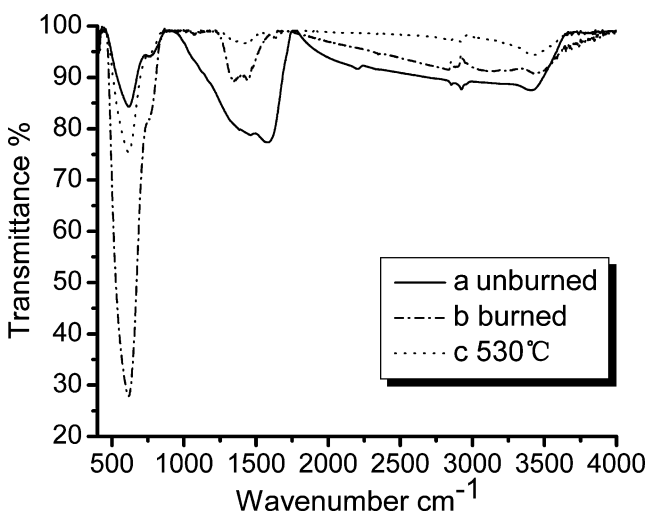


Fig. 3 IR spectra of calcined powders. (a) Unburned powder (b) burned powder at 380 °C for 3 h (c) calcined powder at 530 °C for 3 h

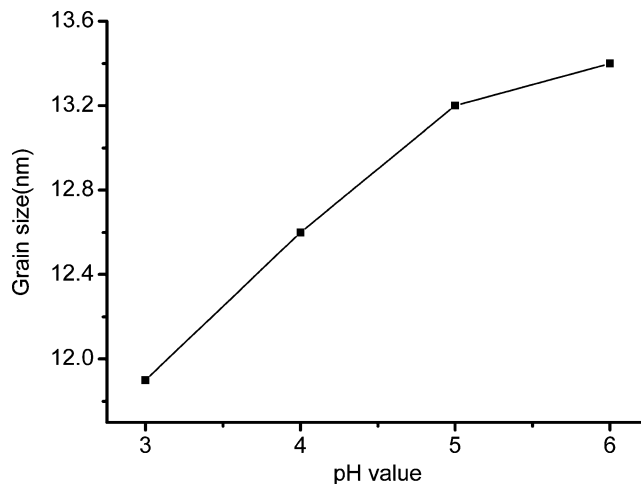


Fig. 4 pH value dependence of grain sizes (powder of $0.36\text{BiScO}_3 - 0.64\text{PbTiO}_3$ in MPB and calcined at 600 °C for 3 h)

The holding time effect on grain size is not as significant as calcining temperature. The grain sizes for $0.38\text{BiScO}_3 - 0.62\text{PbTiO}_3$ powders in rhombohedral phase are 13.0, 14.8 and 15.2 nm when they were calcined for 3, 8 and 16 h. However, there was still a grain growth when the powder was calcined for a long time.

Powders with different components and prepared by the same process show similar trends in calcining temperature and holding time dependences of grain sizes. The calculated results show that powder in rhombohedral phase has larger grain size than that in tetragonal phase.

4 Summary

Different factors which may affect the grain size of BSPT ceramic powders are studied in this work. Though the

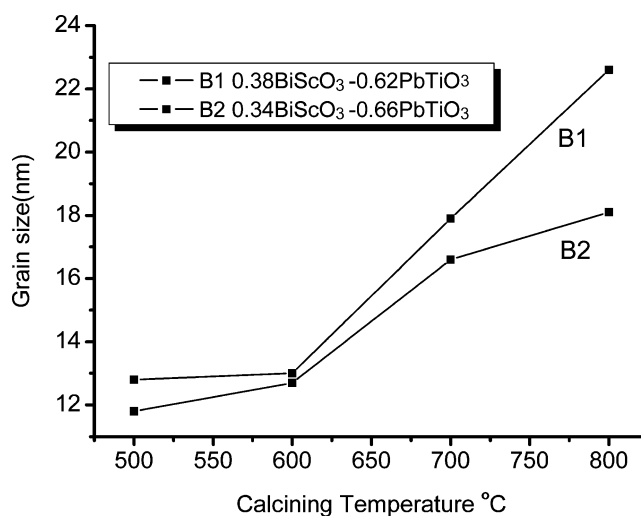


Fig. 5 Calcining temperature dependence of grain sizes. (B1 stands for $0.38\text{BiScO}_3 - 0.62\text{PbTiO}_3$ in rhombohedra phase and B2 stands for $0.34\text{BiScO}_3 - 0.66\text{PbTiO}_3$ in tetragonal phase and they were calcined for 3 h)

preparing method of the solution is an important factor to determine the grain size, there are too many complications such as the formation of metal citrate and polymer molecules that may further affect the grain size. For it is very difficult to quantify the relation between those complications and the grain size, we fix our preparation process in one way and do not change the condition until the final solution was prepared. The results show that the pH value of the final solution, the calcining temperature and the holding time are important factors to determine the grain sizes. Among the three factors, the calcining temperature is the foremost one. Since the grain sizes of those powders are so small that only a subtle change of the sizes could result in variation of different characters, such as the required sintering temperatures. Cursory conclusion is that the powders calcined at 600 °C for 3 h with grain size of 13 nm can be sintered at 1000 °C and using powders with grain size about 3 nm bigger than that would require the sintering temperature increasing by 30 °C. Piezoelectric property was measured to confirm the size effect in the ceramics. The d_{33} of the small-grain ceramics in MPB is enhanced to 530 pC/N comparing to 450 pC/N of large-grain ceramics.

Acknowledgement This work was supported by the Ministry of Science and Technology of China through 973 project under grant

2002CB613301 and National Natural Science Foundation of China under grant 50472006.

This project is (partly) supported by National Center for Nanoscience and Technology, China.

References

1. R.E. Eitel, C.A. Randall, T.R. Shrout, P.W. Rehrig, W. Hackenberger, S.-E. Park, *Jpn. J. Appl. Phys. Part 1* **40**(10), 5999–6002 (2001)
2. C.A. Randall, R.E. Eitel, T.R. Shrout, D.I. Woodward, I.M. Reaney, *J. Appl. Phys.* **93**(11), 9271–9274 (2003)
3. J. Iniguez, D. Vanderbilt, L. Bellaiche, *Phys. Rev. B* **67**, 224107 (2003)
4. R.E. Eitel, C.A. Randall, T.R. Shrout, S.-E. Park, *Jpn. J. Appl. Phys., Part 1* **41**(4A), 2099–2104 (2002)
5. Y. Inaguma, A. Miyaguchi, M. Yoshida, T. Katsumata, Y. Shimojo, R.P. Wang, T. Sekiya, *J. Appl. Phys.* **95**(1), 231–235 (2004)
6. S.J. Zhang, C.A. Randall, T.R. Shrout, *Jpn. J. Appl. Phys. Part 2—Letters* **42**(10A), 1152–1154 (2003)
7. J. Ryu, S. Priya, C. Sakaki, K. Uchino, *Jpn. J. Appl. Phys. Part 1* **41**(10), 6040–6044 (2002)
8. T. Yoshimura, S. Trolier-McKinstry, *Appl. Phys. Lett.* **81**(11), 2065–2066 (2002)
9. H. Huang, C.Q. Sun, T.S. Zhang, P. Hing, *Phys. Rev. B* **63**, 184112 (2001)